Cell Reports, Volume *29*

Supplemental Information

The Classical Complement Pathway Mediates Microglia-Dependent Remodeling of Spinal Motor Circuits during Development and in SMA

Aleksandra Vukojicic, Nicolas Delestrée, Emily V. Fletcher, John G. Pagiazitis, Sethu Sankaranarayanan, Ted A. Yednock, Ben A. Barres, and George Z. Mentis

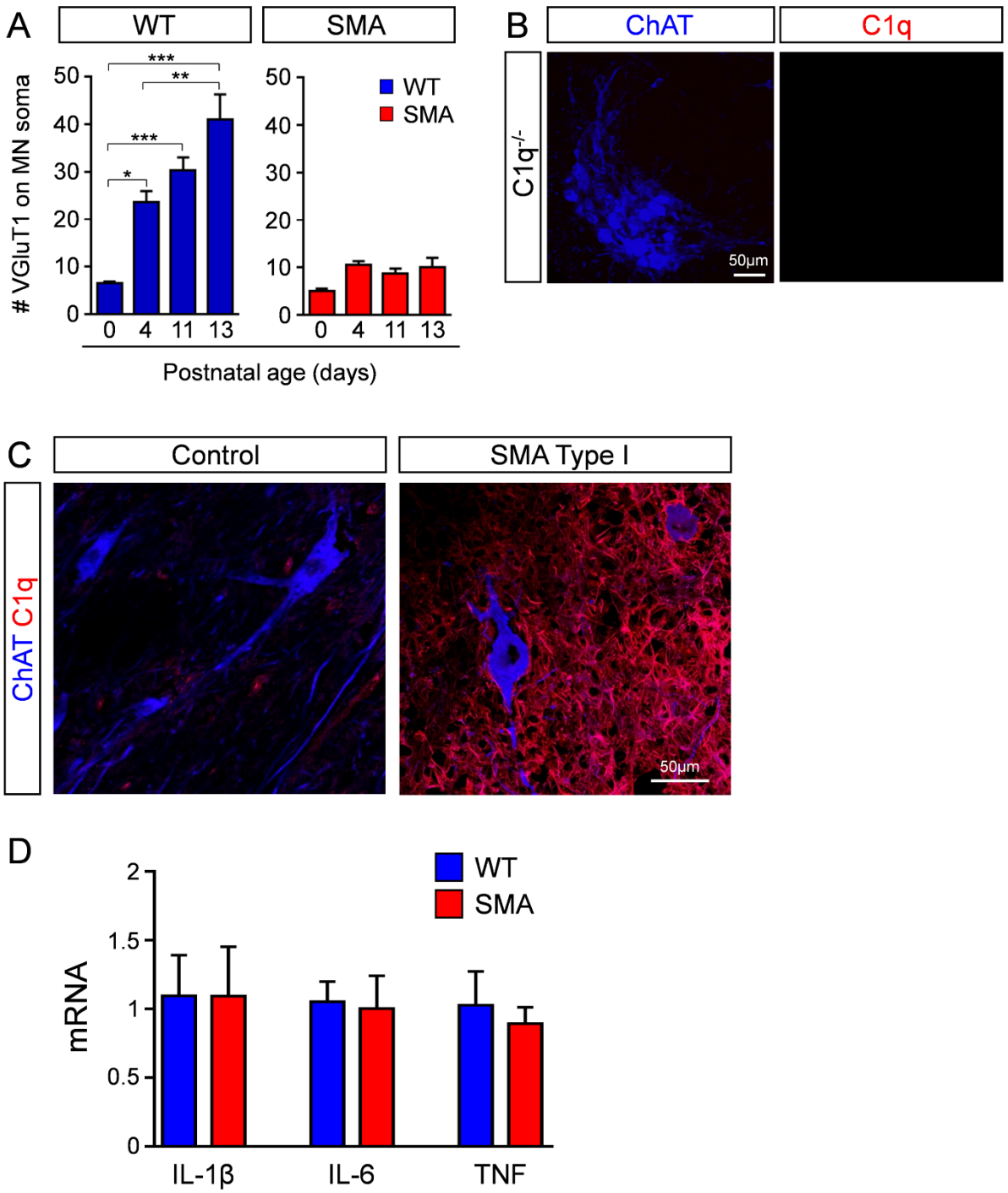

Figure S1 (Related to Figure 1). Temporal difference in the number of VGluT1 synapses on L1 motor neurons in WT and SMA mice; validation of C1q antibody in C1q$^{-/-}$ mice; increased C1q expression in SMA Type I human spinal cord; expression of proinflammatory cytokines in WT and SMA mice at the onset of disease. (A) The total number of VGluT1 synapses on the somata of L1 motor neurons in WT (blue) and SMA (red) mice at P0, P4, P11 and P13. * $p<0.05$, ** $p<0.001$, *** $p<0.001$ with One-way ANOVA and Tukey's test. **(B)** Z-

stack projection of confocal images for validation of C1q antibody in the spinal cord of C1q-/- mice (ChAT in blue and C1q in red). (Total distance in z-axis: 9.1 μm). **(C)** Z-stack projection of confocal images with ChAT (blue) and C1q (red) immunoreactivity from post-mortem control and SMA patient's lumbar spinal cord segment (total distance in z-axis: 6μm). **(D)** RT-qPCR analysis of IL-1β, IL-6 and TNF mRNA levels in the L1-L2 spinal cord segments of WT (n=3) and SMA (n=3) mice at P4. No significant difference was observed, t-test.

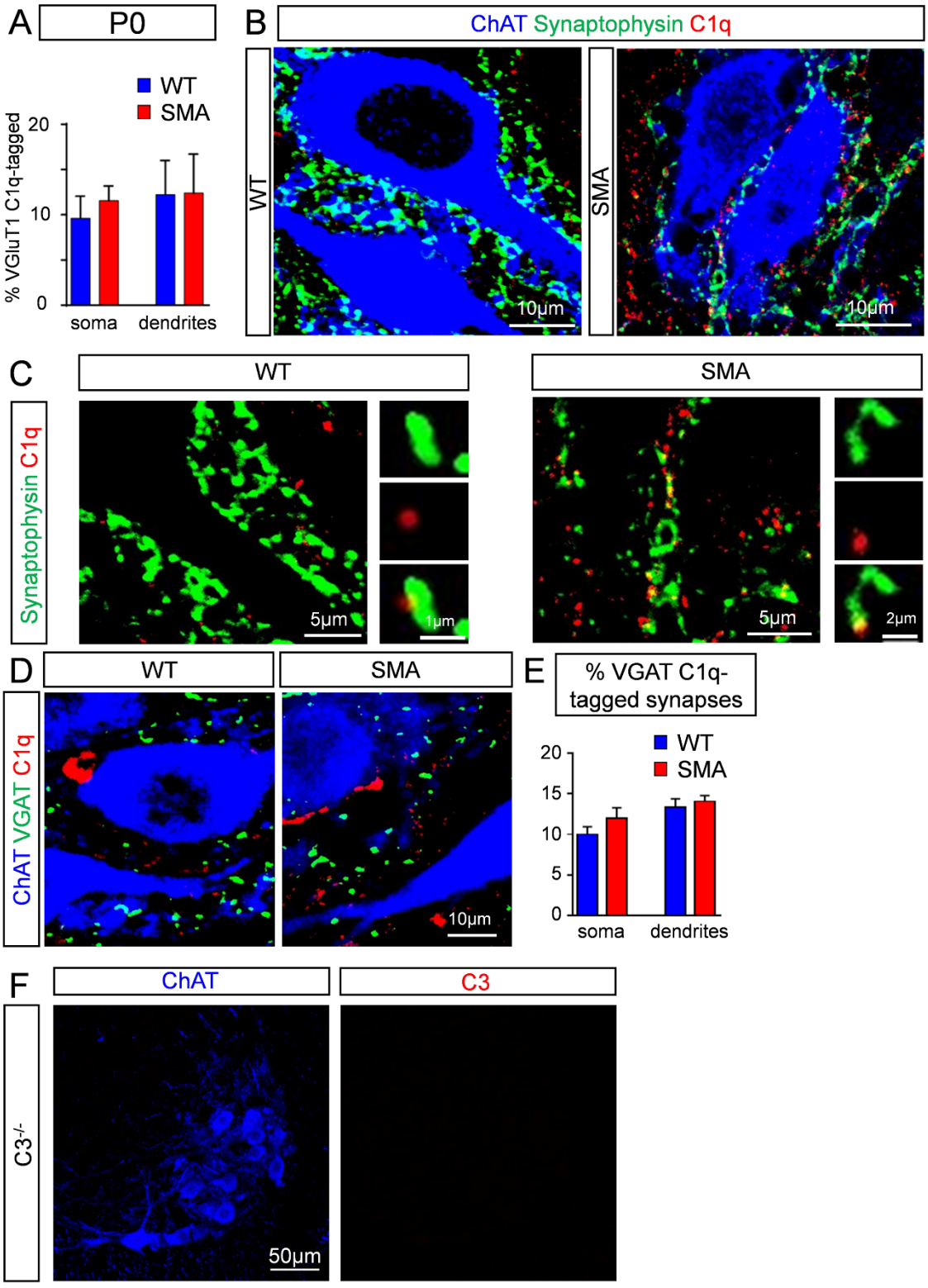

Figure S2 (Related to Figure 2). C1q-tagging at different ages and different types of synapses; C3 antibody specificity. (A) Percentage of VGluT1 C1q-tagged synapses on the somata and dendrites of L1 WT (454

synapses from 56 MNs) and SMA (487 synapses from 46 MNs) motor neurons at birth (P0). **(B)** Confocal images of ChAT (blue), Synaptophysin (green) and C1q (red) in WT and SMA motor neurons at P4. **(C)** Higher magnification confocal images of synaptophysin (green) and C1q (red) in WT and SMA spinal cords. **(D)** Confocal images of ChAT (blue), VGAT (green) and C1q (red) in WT and SMA motor neurons at P4. **(E)** Percentage of VGAT C1q-tagged synapses on the somata and dendrites of L1 WT (n=55) and SMA (n = 29) motor neurons at P4. **(F)** Z-stack projections of confocal images of ChAT (blue) and C3 (red) in $C3^{-/-}$ L1 motor neurons at P4 (Total distance in z-axis: 9.1 μm).

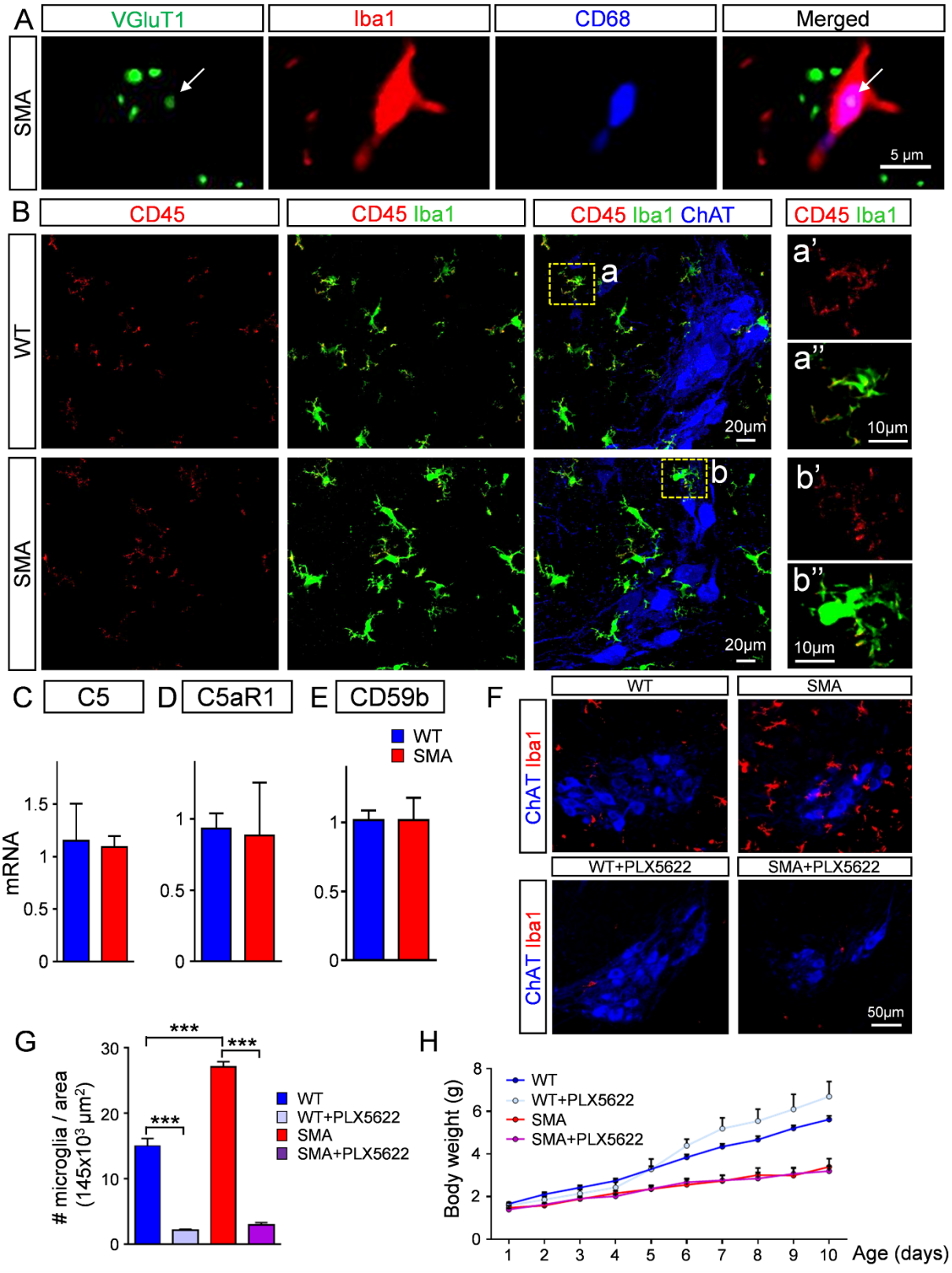
A
VGluT1
Iba1
CD68
Merged
SMA
5 μm
B
CD45
CD45 Iba1
CD45 Iba1 ChAT
CD45 Iba1
WT
SMA
a
a'
a''
b
b'
b''
20μm
10μm
C
C5
D
C5aR1
E
CD59b
WT
SMA
mRNA
F
WT
SMA
ChAT Iba1
WT+PLX5622
SMA+PLX5622
50μm
G
microglia / area (145x10³ μm²)
***
WT
WT+PLX5622
SMA
SMA+PLX5622
H
Body weight (g)
Age (days)

Figure S3 (Related to Figure 3). Microglia eliminate VGluT1 synapses; expression of CD45 in WT and SMA mice; expression of C5, C5Ar1 and CD59b in WT and SMA mice; Plexxikon-5622 depletes microglia but doesn't affect body weight of treated pups. (A) Single optical plane confocal images of SMA L1 microglia within the motor neuron nucleus, visualized by Iba1 (red) and CD68 (blue) as well as VGluT1 (green) immunoreactivity at P4. Arrow indicates VGluT1 signal within microglial lysosome. **(B)** Z-stack projections of confocal images of WT and SMA L1 spinal cords visualized by CD45 (red), Iba1 (green), ChAT (blue) at P4 (total distance 5.4 μm). Dotted boxes are shown at higher magnification on right side for CD45 (red, a') and CD45 (red, a'') and Iba1 (green, a'') immunoreactivity in WT and in SMA (b', b''). RT-qPCR analysis of C5 **(C)**, C5aR1 **(D)** and CD59b **(E)** mRNA levels in the L1-L2 spinal cord segments of WT (n=3) and SMA (n=3) mice at P4. No significant difference was observed, t-test. **(F)** Confocal images of ChAT (blue) and Iba1 (red) in WT, SMA, WT+PLX5622 and SMA+PLX5622 motor neuron nuclei at P11. **(G)** Total number of microglia (Iba1+ cells) per $145x10^3$ μm^2 area (within motor neuron area) in WT (n=5), WT+PLX5622 (n=3), SMA (n=7) and SMA+PLX5622 (n=3) mice at P11. *** $p<0.001$, One-way ANOVA, with Tukey's test. **(H)** Body weights for WT (n=10), WT+PLX5622 (n=9), SMA (n=8) and SMA+PLX5622 (n=18) mice.

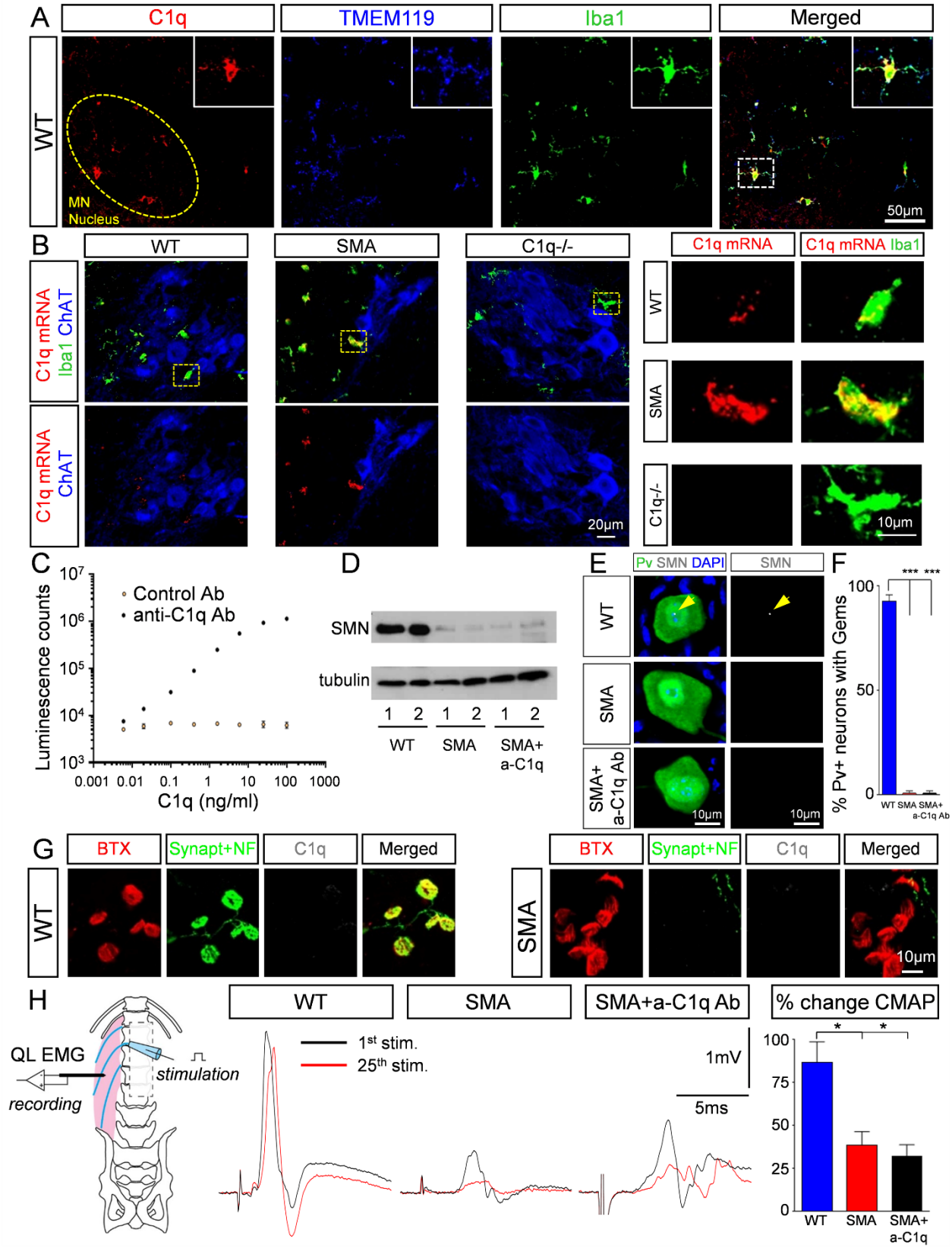
A
C1q
TMEM119
Iba1
Merged
WT
MN
Nucleus
50μm
B
WT
SMA
C1q-/-
C1q mRNA
Iba1 ChAT
C1q mRNA
ChAT
20μm
C1q mRNA
C1q mRNA Iba1
WT
SMA
C1q-/-
10μm
C
Control Ab
anti-C1q Ab
Luminescence counts
C1q (ng/ml)
D
SMN
tubulin
1 2 1 2 1 2
WT
SMA
SMA+
a-C1q
E
Pv SMN DAPI
SMN
WT
SMA
SMA+
a-C1q Ab
10μm
10μm
F
% Pv+ neurons with Gems
WT SMA SMA+
a-C1q Ab
G
BTX
Synapt+NF
C1q
Merged
WT
SMA
10μm
H
QL EMG
recording
stimulation
WT
SMA
SMA+a-C1q Ab
1st stim.
25th stim.
1mV
5ms
% change CMAP
WT
SMA
SMA+
a-C1q

Figure S4 (Related to Figure 4). Microglia are the source of C1q in the spinal cord, binding specificity of anti-C1q antibody and its isotype control; *in vivo* treatment with anti-C1q results in no upregulation of SMN protein and no effect on NMJ denervation. (A) Single optical plane confocal images of C1q (red), TMEM119 (blue), Iba1 (green) in WT mice at P4. Circled area indicates approximate location of motor neuron nucleus. Dotted box indicates area shown in insets at higher magnification with colocalization of microglia (Iba1+/TMEM119+ cells) and C1q. **(B)** Single optical plane confocal images from *in situ* C1q mRNA (red) combined with Iba1 (green) and ChAT (blue) immunoreactivity in WT, SMA and $C1q^{-/-}$ mice at P4. Dotted boxes are shown at higher magnification on right side for C1q mRNA (red) and Iba1 (green) immunoreactivity in WT, SMA and $C1q^{-/-}$ mice. **(C)** C1q binding assay – ELISA of anti-C1q neutralizing antibody (black), and Isotype control antibody (yellow) to human C1q. **(D)** Western blot analysis for SMN and β-tubulin protein expression from two WT, two SMA and two SMA+a-C1q Ab spinal cords (L1-L3) at P11. **(E)** Confocal images of Parvalbumin (green), SMN (white) and DAPI (blue) in WT, SMA and SMA+a-C1q Ab DRGs at P11. Arrow indicates presence of gem, visualized by SMN (white). **(F)** Percentage of parvalbumin neurons with gems in WT (n=50), SMA (n=50) and SMA+a-C1q Ab (n=50) DRGs at P11. *** $p<0.01$, One-way ANOVA with Tukey's test. **(G)** Z-stack projections of confocal images of α-bungarotoxin (BTX, red), synaptophysin and neurofilalment (green) and C1q (white) in NMJs from the QL muscle in WT and SMA mice at P5 (Total distance: 7 μm). **(H)** Schematic illustration of experimental *ex vivo* setup for assessment of Compound Muscle Action Potentials (CMAPs) in the Quadratus Lumborum muscle in mice. Superimposed traces of the 1^{st} (black) and 25^{th} (red) CMAPs during 25 Hz stimulation of the L2 ventral root in WT, SMA and SMA+a-C1qAb mice. Graph shows the percentage change in baseline-to-peak CMAP amplitude of the 25^{th} response normalized to the 1^{st} CMAP following 25 Hz stimulation of the ventral root in WT (n=5), SMA (n=5) and SMA+a-C1qAb (n=5) mice. * $p<0.05$, One-way ANOVA with Tukey's test.

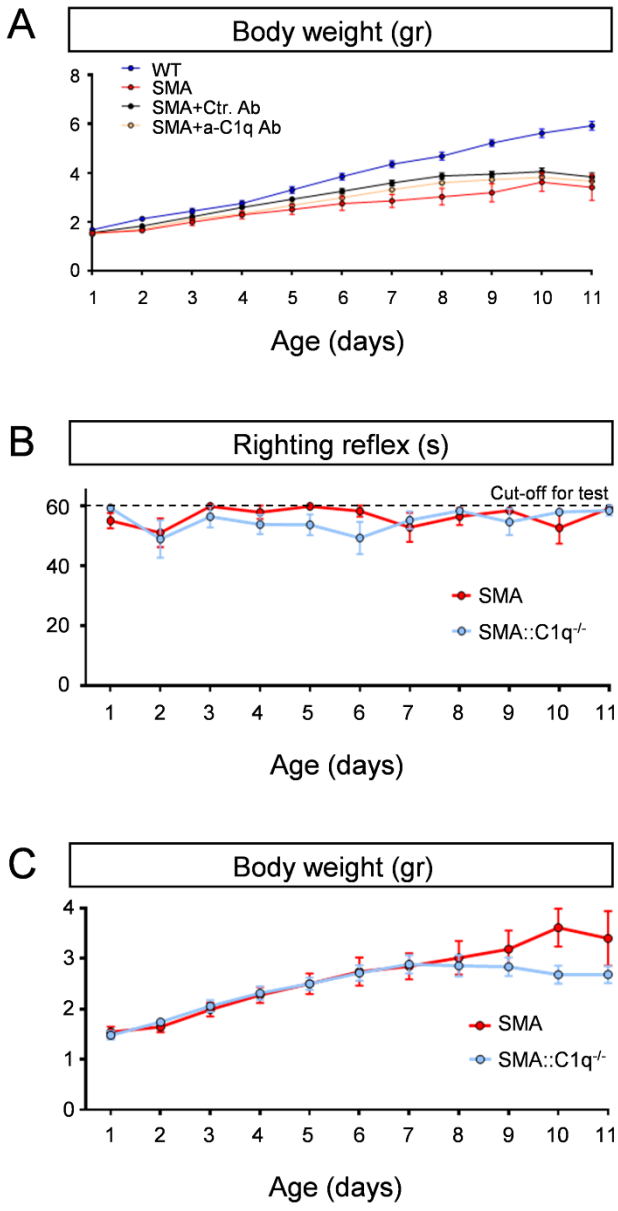

Figure S5 (Related to Figure 5). a-C1q and isotype control antibody treatment effect on body weight; genetic deletion of C1q does not confer behavioral benefits in SMA mice. (G) Body weights gain in WT (blue), SMA (red), SMA+Ctr. Ab (black) and SMA+a-C1q Ab (orange) mice. Righting time **(B)** and body weight gain **(C)** during postnatal development in SMA (n=9) and SMA::C1q$^{-/-}$ (n=10) mice.

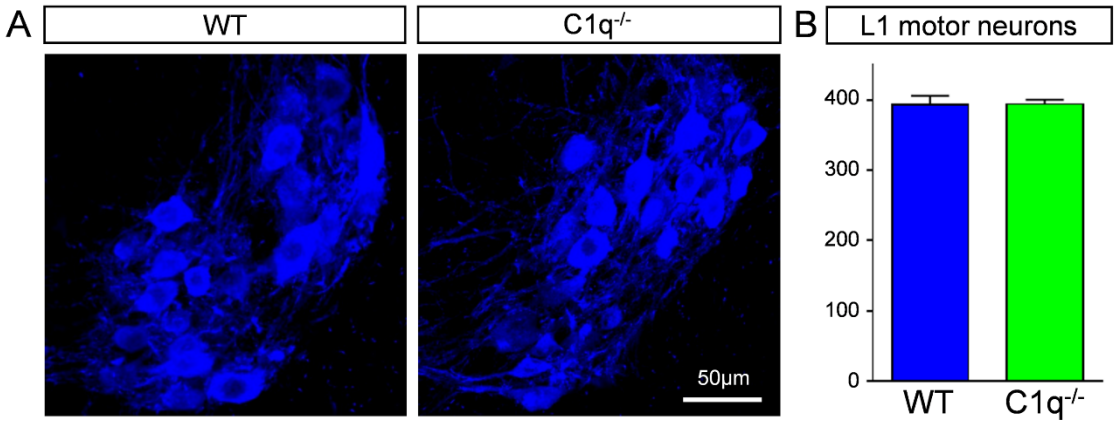

Figure S6 (Related to Figure 6). Genetic deletion of C1q does not result in any motor neuron death in wild type mice. (A) Confocal images of ChAT+ L1 motor neurons in WT and C1q-/- mice at P11. **(B)** The total number of L1 motor neurons in WT and C1q$^{-/-}$ mice.

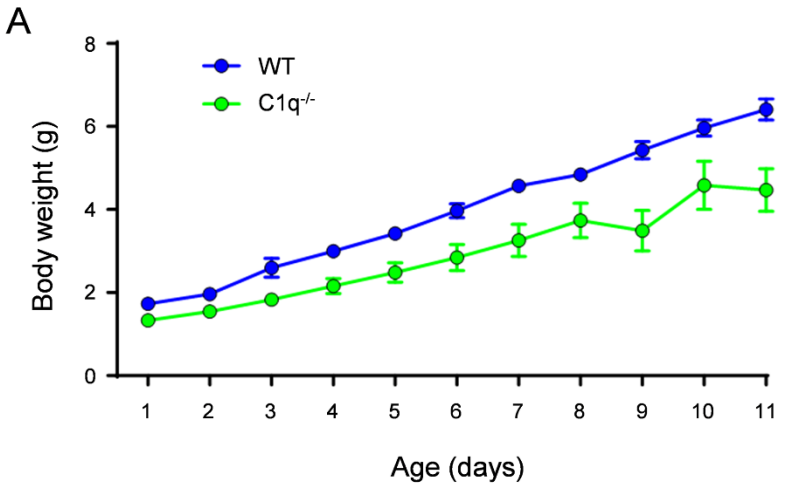

Figure S7 (Related to Figure 7). Genetic deletion of C1q results in mild under weight gain in WT background mice. (A) Body weight gain in WT (n=10) and C1q$^{-/-}$ (n=10) mice.

Table S1. Primers for Real time RT-qPCR (related to STAR Methods).

C1qA forward primer:	AAGGATGGGGCTCCAGGAAAT
C1qA reverse primer:	TTCCCCTGGGTCTCCTTTAAAACCT
C3 forward primer:	CCATCACAGTCCGCACCAAGAA
C3 reverse primer:	GAGTTGTGCATAGTGCTGTAGGGA
GAPDH forward primer:	AATGTGTCCGTCGTGGATCTGA
GAPDH reverse primer:	GATGCCTGCTTCACCACCTTCT
C5 forward primer:	CAGTAACAGTCACAGAATCTTCAGGT
C5 reverse primer:	GGAGAGAGGACATATTTGACTCCA
C5aR1 forward primer:	CCAGGACATGGACCCCATAGATA
C5aR1 reverse primer:	CCATCCGCAGGTATGTTAGGA
CD59b forward primer:	TCTCTATGCTGTAGCCGGAAG
CD59b reverse primer:	TTGTATGCCTGCCACGTCTA
IL-1β forward primer:	AGTTGACGGACCCCAAAAG
IL-1β reverse primer:	AGCTGGATGCTCTCATCAGG
IL-6 forward primer:	AGTCCGGAGAGGAGACTTCA
IL-6 reverse primer:	GCCATTGCACAACTCTTTTCTCA
TNF forward primer:	GTCCCCAAAGGGATGAGAAGTT
TNF reverse primer:	TGTGAGGGTCTGGGCCATAG